

The scattered disc of HR 8799

Fabian Geiler¹, Alexander V. Krivov¹, Mark Booth¹, and Torsten Löhne¹

¹ *Astrophysikalisches Institut und Universitätssternwarte, Friedrich-Schiller-Universität Jena, Schillergäßchen 2–3, 07745 Jena, Germany*

Received 31 August 2018; accepted 21 November 2018

ABSTRACT

HR 8799 is a young F0-type star with four directly imaged giant planets and two debris belts, one located exterior and another one interior to the region occupied by the planetary orbits. Having an architecture similar to that of our Solar System, but also revealing dissimilarities such as high masses of planets, a huge radial extent and a high mass of the outer debris belt, HR 8799 is considered to be a benchmark to test formation and evolution models of planetary systems. Here we focus on the outer debris ring and its relation to the planets. We demonstrate that the models of the outer disc, proposed previously to reproduce Herschel observations, are inconsistent with the ALMA data, and vice versa. In an attempt to find a physically motivated model that would agree with both observational sets, we perform collisional simulations. We show that a narrow planetesimal belt and a radiation pressure induced dust halo cannot account for the observed radial brightness profiles. A single, wide planetesimal disc does not reproduce the data either. Instead, we propose a two-population model, comprising a Kuiper-Belt-like structure of a low-eccentricity planetesimal population (“the classical Kuiper Belt”) and a high-eccentricity population of comets (“scattered disc”). We argue that such a structure of the exo-Kuiper belt of HR 8799 could be explained with planet migration scenarios analogous to those proposed for the Kuiper Belt of the Solar System.

Key words: planets and satellites: formation – circumstellar matter – stars: individual: HR 8799 – Kuiper Belt: general

1 INTRODUCTION

Debris discs, consisting of planetesimal remnants of the protoplanetary disc, are a vital component of the study of planet formation. Studies have shown that many discs coexist with planets (Maldonado et al. 2012; Wyatt et al. 2012; Eiroa et al. 2013; Marshall et al. 2014; Moro-Martín et al. 2015; Meshkat et al. 2017). One such system is HR 8799, an F0V (Gray et al. 2003) star located 41.29 ± 0.15 pc (Gaia Collaboration et al. 2018) away from Earth with four directly imaged giant planets at projected distances of 27, 43, 68, and 15 AU (Marois et al. 2008, 2010). Additionally warm dust (6–10 AU) and a Kuiper Belt analogue (> 100 AU) have been detected (Sadakane & Nishida 1986; Su et al. 2009; Hughes et al. 2011; Matthews et al. 2014; Booth et al. 2016). This combination of objects in one system has made HR 8799 the centre of many dynamical studies and stability analyses (e.g. Reidemeister et al. 2009, Fabrycky & Murray-Clay 2010, Goździewski & Migaszewski 2009, Marois et al. 2010, Goździewski & Migaszewski 2014, Goździewski & Migaszewski 2018). Not only is the stability of the system of great interest, the formation of these objects is also puzzling. The two leading models for giant gas planet formation are core accretion (Pollack et al. 1996; Kenyon & Bromley 2009) and formation through gravitational instability in the protoplanetary disc (Boss 1997). Neither of these can explain the wide orbits and high masses of these planets (Marois et al. 2010; Currie et al. 2011) without including additional mechanisms such as migration

(Crida 2009) and planet-planet scattering (Chatterjee et al. 2008). A further question is which role the debris disc may have played in the evolution of the system. It might have circularised the orbits of scattered planets or facilitated migration (Moore et al. 2013).

An analysis of the entire HR 8799 system is necessary to understand how this planetary system has formed and evolved. Many attempts were made to better observe, model or explain the structure of the debris disc. While both Su et al. (2009) and Matthews et al. (2014) set the inner edge of the outer disc at roughly 100 AU, Booth et al. (2016) found it to be at 145 AU. The latter implies a large gap between HR 8799b and the inner edge. The opening of such a wide gap can be explained with the chaotic zone of a planet which depends on the mass, position (Wisdom 1980; Duncan et al. 1989) and eccentricity of the planet (Pearce & Wyatt 2014). In the chaotic zone, mean motion resonances overlap and orbits become unstable, thus particles are removed from the system on short dynamical timescales. The outermost known planet HR 8799 b can create such a zone up to 110 AU, which is sufficient for the inner edge inferred by Matthews et al. (2014). Assuming an eccentricity of at least 0.3 was held by the planet for a long time, planet b can even clear the system up to 145 AU (Moro-Martín et al. 2010). As an alternative way to explain this gap, Booth et al. (2016) propose a fifth planet positioned at 110 AU with a mass of $1.25 M_{\text{Jup}}$. If farther out or on an orbit with higher eccentricity, the mass of the planet can also be lower.

The cold belt is found to extend to around 300 AU in the models of [Su et al. \(2009\)](#) and [Matthews et al. \(2014\)](#), who also find emission extending out to 2000 AU, which they attribute to small grains being blown out by radiation pressure. In the ALMA data, however, this extended emission is not visible and the cold belt is seen to extend to 450 AU ([Booth et al. 2016](#)). A challenge for both observations is to explain why the disc is so extended and still sufficiently excited. The excitation models of [Kenyon & Bromley \(2008\)](#) need Pluto sized objects to stir the disc, but the formation of these objects at the distance of the cold disc of HR 8799 would take longer than the age of the system. Even assuming smaller objects sufficiently stir the disc, self stirring is still not able to produce destructive collisions in the extended disc ([Krivov & Booth 2018](#)). This poses the question of how to explain any sort of destructive collision at these distances. So either this extended disc is still primordial ([Heng & Tremaine 2010](#); [Krivov et al. 2013](#)) or the stirring has to be attributed to another mechanism, such as stirring by planets.

The previous studies of HR 8799’s debris disc, however, utilized ad hoc distributions of dust and not a collisional model. The goal of this work is to find a model which can explain the appearance of HR 8799’s outer massive debris disc in both the Herschel/PACS ([Poglitsch et al. 2010](#)) and the ALMA ([Brown et al. 2004](#)) observations, and how it might be related to the planets.

In section 2 we focus on the system itself and the observations we used. In section 3 our methods are discussed. In section 4 we present the modelled configurations. Section 5 discusses the results and their implications for the formation history of the system. Finally we present our conclusions in section 6.

2 PREVIOUS MODELS

Many observations have already peered into the architecture of HR 8799, giving us a detailed image of the system. The infrared excess was discovered by IRAS ([Sadakane & Nishida 1986](#); [Zuckerman & Song 2004](#); [Rhee et al. 2007](#)), a warm inner component was observed by Spitzer/IRS ([Jura et al. 2004](#); [Chen et al. 2006](#); [Su et al. 2009](#)) and lastly four giant planets were directly imaged by the Keck and Gemini telescopes ([Marois et al. 2008, 2010](#)). Here we focus primarily on the observations of [Matthews et al. \(2014\)](#) and [Booth et al. \(2016\)](#), because they resolved the cold disc, with Herschel/PACS and ALMA respectively, at wavelengths dominated by the cold disc emission. From the former we used the 70 and 100 μ m observations, neglecting the 160 μ m and the additional SPIRE data, as these were strongly affected by emission from a background cloud and their resolution is poorer. From the latter we got 1.34mm observations, giving us high resolution images at a much longer wavelength and helping us constrain the location of the bigger grains and their parent bodies, the planetesimals.

In both [Matthews et al. \(2014\)](#) and [Booth et al. \(2016\)](#) parametric models of the surface brightness distribution were fit to the observed profiles. In order to determine how well the model designed to fit the Herschel data does at fitting the the ALMA data and vice versa, we start by reproducing these models, albeit using physically motivated models. In other words, we distribute the dust according to the parameters given in those models but use realistic grain properties and a size distribution. Unless stated otherwise, the populations consisted of μ m to km sized objects distributed between the inner and outer edge of the disc following a size distribution of $m^{-1.87}$. The material, used throughout this work, is a mixture of astrosilicate (50%, [Draine 2003](#)), ice ([Li & Greenberg](#)

Table 1. Photometry of HR 8799

| Photometric Band | Magnitude [mag] | Remarks | Ref. |
|-----------------------|----------------------|---------|------|
| B | 6.090 ± 0.300 | | (1) |
| B | 6.196 | | (2) |
| B | 6.210 ± 0.010 | | (3) |
| B | 6.214 ± 0.009 | | (4) |
| V | 5.960 ± 0.010 | | (4) |
| V | 5.959 | | (2) |
| V | 5.960 ± 0.010 | | (3) |
| I | 5.690 ± 0.300 | | (1) |
| J | 5.383 ± 0.027 | | (5) |
| H | 5.280 ± 0.018 | | (5) |
| K _S | 5.240 ± 0.018 | | (5) |
| Wavelength [μ m] | Flux [mJy] | | |
| 9 | 404.035 ± 17.808 | (a) | (6) |
| 12 | 278 ± 26 | (b) | (7) |
| 12 | 267 ± 25 | (b) | (8) |
| 18 | 120.533 ± 80.276 | (c) | (6) |
| 23.68 | 86.6 ± 1.7 | (d) | (9) |
| 60 | 445 ± 70 | (e) | (8) |
| 60 | 450 ± 71 | (e) | (7) |
| 60 | 412 ± 21 | | (10) |
| 71.42 | 610 ± 31 | | (9) |
| 70 | 537 ± 15 | (f) | (11) |
| 90 | 585 ± 41 | | (10) |
| 90 | 488.632 ± 74.838 | (g) | (12) |
| 100 | 687 ± 20 | (f) | (11) |
| 155.89 | 555 ± 66 | | (9) |
| 160 | 570 ± 50 | (f) | (11) |
| 250 | 309 ± 30 | (f) | (11) |
| 350 | 163 ± 30 | (f) | (11) |
| 350 | 89 ± 26 | | (13) |
| 500 | 74 ± 30 | (f) | (11) |
| 850 | 10.3 ± 1.8 | | (14) |
| 850 | 17.4 ± 1.5 | | (15) |
| 1200 | 4.8 ± 2.7 | | (16) |

Remarks: (a) color corrected 7000K = 1.184 (b) color corrected 5000K = 1.43 (c) color corrected 7000K = 0.990 (d) calibrated with [Brott & Hauschildt \(2005\)](#) model 7400 K (e) color corrected 50K = 0.91; (f) BG source subtracted; (g) color corrected 50K = 0.979

References: (1) The USNO-B1.0 Catalogue ([Monet et al. 2003](#)); (2) NOMAD Catalogue ([Zacharias et al. 2004](#)), from Tycho-2 Catalogue ([Høg et al. 2000](#)); (3) The Guide Star Catalogue Version 2.3.2 ([Lasker et al. 2008](#)); (4) The Hipparcos and Tycho Catalogues ([Perryman et al. 1997](#)); (5) 2MASS All-Sky Catalogue ([Skrutskie et al. 2006](#)); (6) Akari/IRC Mid-Infrared All-Sky Survey Point Source Catalogue ([Ishihara et al. 2010](#)); (7) IRAS Faint Source Catalogue, $|b| > 10^\circ$, Version 2.0 ([Moshir et al. 1990](#)); (8) IRAS Catalogue of Point Sources, Version 2.0 ([Helou & Walker 1988](#)); (9) ([Su et al. 2009](#)); (10) ([Moór et al. 2006](#)); (11) ([Matthews et al. 2014](#)); (12) Akari/FSI All-Sky Survey Point Source Catalogues ([Yamamura et al. 2010](#)); (13) ([Patience et al. 2011](#)); (14) ([Williams & Andrews 2006](#)); (15) SONS-Survey ([Holland et al. 2017](#)); (16) ([Sylvester et al. 1996](#))

Table 2. Initial parameters of some proposed disc components and our preferred model.

| Parameter | Dust Distr. Model Matthews+14 | Dust Distr. Model Booth+16 | Excited disc | Wide Cold disc | Preferred Model |
|-----------------------|----------------------------------|-------------------------------|--------------|----------------|-----------------|
| <i>1st Population</i> | | | | | |
| $M [M_{\oplus}]$ | 5.9 | 42 | - | 220 | 134 |
| $a [AU]$ | 100 – 310 | 145 – 430 | - | 150 – 440 | 140 – 440 |
| e | - | - | - | 0 – 0.1 | 0 – 0.1 |
| γ | 1.0 | 0.6 | - | 0.6 | 1.0 |
| <i>2nd Population</i> | | | | | |
| $M [M_{\oplus}]$ | 0.08 | - | 220 | - | 67 |
| $a [AU]$ | 310 – 2000 | - | 360 – 440 | - | 360 – 440 |
| e | - | - | 0.5 – 0.6 | - | 0.3 – 0.5 |
| γ | 1.7 | - | 1.0 | - | 1.0 |

Notes: a stands for the semimajor axis, e is the eccentricity, and γ is the slope of the radial distribution of the optical depth with the form $r^{-\gamma}$. M stands for the initial mass of the disc. Since the dust distributions models describe observations, their masses reference the current disc.

1998), and vacuum (each 25%) with a density of $\rho = 2.0 \text{ g/cm}^3$, where vacuum is serving as a substitute for porosity. We ended up with “dummy models”, replicas of the ad hoc dust distributions of the other studies, created with our tools, that allowed us to extrapolate from the original to other wavelengths. We note that, due to the difference in modelling technique, we cannot exactly reproduce the models of the previous models, but our representations are close enough to make qualitative comparisons.

To create the corresponding images, the distribution of the dust and the material properties were taken into account and the thermal emission calculated. These artificial images were then convolved with a Gaussian Beam corresponding to the point spread functions (PSF) of the instruments. We used normalized elliptical Gaussians with sizes of $5.8'' \times 5.5''$ for the $70\mu\text{m}$ images, $6.9'' \times 6.7''$ for the $100\mu\text{m}$ images and $1.3'' \times 1.7''$ for the $1340\mu\text{m}$ images. From these images we calculated the azimuthally averaged radial profiles and compare them to the deprojected radial profiles of the observations.

In addition to comparing our models to these profiles, we also compare them to the full SED. All of the photometry for the HR 8799 system available in the literature is presented in Table 1. We used the standard calibration system of Johnson, to transform the B , V , I magnitudes into flux values for the spectral energy distribution (SED). The J , H and K_S magnitudes from 2MASS were transformed with the calibrations of Cohen et al. (2003). In order to model the stellar component we use data from the PHOENIX model (Brott & Hauschildt 2005) fitted by Matthews et al. (2014).

In the following we discuss the extrapolated models of Matthews et al. (2014) and Booth et al. (2016).

2.1 Disc with halo

In the PACS observations the disc extends from 100 – 310 AU, but shows a halo stretching to 2000 AU (see Tab. 2). Distances of up to 2000 AU are unlikely to be reached by planetesimals, therefore small grains spread by radiation pressure (Krivov et al. 2006) are the most plausible explanation. Furthermore, Matthews et al. (2014) noted differences in the temperatures of the main belt and halo when considering $24\mu\text{m} + 70\mu\text{m}$ compared to $70\mu\text{m} + 100\mu\text{m}$ data. This suggests two distinct populations of grains being present.

The slopes of the surface brightness profiles in Matthews et al. (2014) differ from wavelength to wavelength, but since we utilize

the geometrical normal optical depth distributions and not the surface brightness, we do not need to choose different radial slopes for different wavelengths. Instead we use the position of the belt, as given in Matthews et al. (2014), but assume a single slope for the optical depth at all wavelengths that best mimicks the slope of the radial profiles (see Tab. 2). The minimum grain size of the halo is set to the blowout limit of $s_{\text{blow}} \approx 3\mu\text{m}$ (Burns et al. 1979) while the maximum grain size in the halo is set to three times that value. Although smaller grains might exist within the halo, their contribution to the radial profiles at wavelengths of $\geq 70\mu\text{m}$ is negligible. One has to point out that in this dummy model (as in the Su et al. 2009 and the Matthews et al. 2014 models) the halo is not created by radiation pressure, but consists of small dust grains distributed to resemble a halo. All other parameters needed are assumed such that our synthetic profiles reproduce the PACS profiles well. We calculate the error bars as the root mean square of the azimuthally averaged flux within annuli of a width of 1 pixel.

This approach, as seen in red in Fig. 1, does reproduce the outer regions of the Herschel observations with a small flux deviation in the $100\mu\text{m}$ profile. In the ALMA profile, however, the synthetic profile peak appears closer to the star while also underpredicting the flux. The peak location is related to the location of the inner edge set by the model. The lack of flux, however, appears to be an inherent problem with the assumption of a small grain halo, as the SED also follows a much too steep slope at longer wavelengths. This result differs from the SED in Matthews et al. (2014) as they fit the photometry data with a modified black body rather than self consistently fitting the images and the SED. Larger grains in the halo could remedy the shortcoming, but it is hard to argue that radiation pressure would transport these grains that far out in the system. So while this offers a solution to the SED shape, the position of the peak in the ALMA profiles remains problematic.

2.2 Extended disc

Booth et al. (2016) observed the disc around HR 8799 at $1340\mu\text{m}$ with ALMA in Band 6. The model they created to fit the observations sets the inner edge of the disc at around 145 AU and the outer one at 430 AU (see Tab. 2). In the observations themselves the disc appears broad but without halo. This means the planetesimals are present everywhere across this distance range, as the longer wavelength is more effective at probing larger grains.

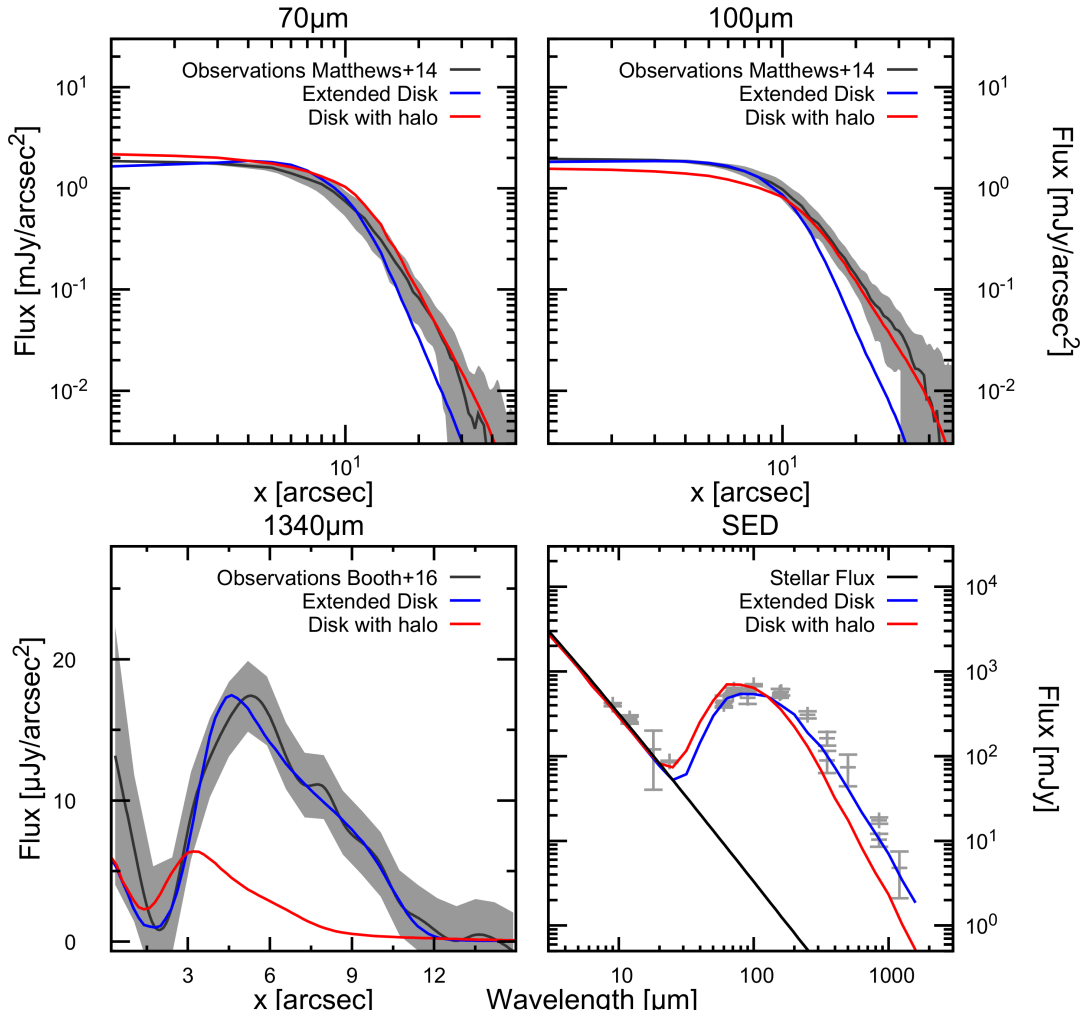


Figure 1. Radial profiles of the disc at 70, 100, 1340 μm and the SED for the system structures proposed in previous works. In black: observations and error bars (in grey). Red: a debris disc from 100 – 310 AU and a halo of small grains out to 2000 AU (as seen in [Matthews et al. \(2014\)](#)). Blue: a debris disc with planetesimals from 145 AU to 430 AU with eccentricities up to 0.1 (as seen in [Booth et al. \(2016\)](#)).

Using the parameters given in [Booth et al. \(2016\)](#) we computed the radial brightness profiles as seen in blue in Fig. 1. Since the model in [Booth et al. \(2016\)](#) was used to explain the ALMA observations, we chose any parameters not given in the publication in such a way, that the ALMA observation was well reproduced by our model. From the resulting dust distribution we calculated images and the SED (see Fig. 1). The model is in good agreement with the ALMA observations. Small differences can be explained with the different approach of generating images. The PACS observations, on the other hand, reveal some clear discrepancies. The profile does not reach out far enough.

3 COLLISIONAL EVOLUTION MODEL

3.1 Collisional Code

In order to construct a physically motivated model of the disc that is consistent with both Herschel and ALMA wavelengths, we use the ACE code ([Krivov et al. 2006](#); [Löhne et al. 2012](#); [Krivov et al. 2013](#)) to model the long term collisional evolution of a dust distribution. We assume an azimuthally symmetrical distribution of planetesimals from submicrometer sizes up to ~ 100 km. Using this as

a starting point, the Smoluchowski–Boltzmann equation is solved to calculate gain and loss of material in this system.

The code uses the pericentric distance, eccentricity and the mass as phase space variables. The inclination and the opening angle are fixed at half the eccentricity. We average the particle densities from the mid-plane to the maximum inclination. If particles enter an unbound orbit, the production rate and dynamical lifetime determine its abundance. The material is considered to have left the system by the next time step and is removed from the simulation.

3.2 Collisional physics

While direct stellar radiation pressure is taken into account, we decided to not consider Poynting–Robertson drag, as test runs have shown that it has little impact on the evolution. Stellar wind drag was also neglected, as F stars such as HR 8799 are not expected to have winds strong enough to influence the disc evolution. The composition was the same as we used for the calculation of the previous models, which was mentioned in section 2.2. Regarding the material strength, we adopted the formula of [Löhne et al. \(2012\)](#), which includes the velocity dependence described by [Stewart & Leinhardt \(2009\)](#). The coefficients $b_s = -0.37$, $Q_{D,s} = 2 \times 10^{-6}$

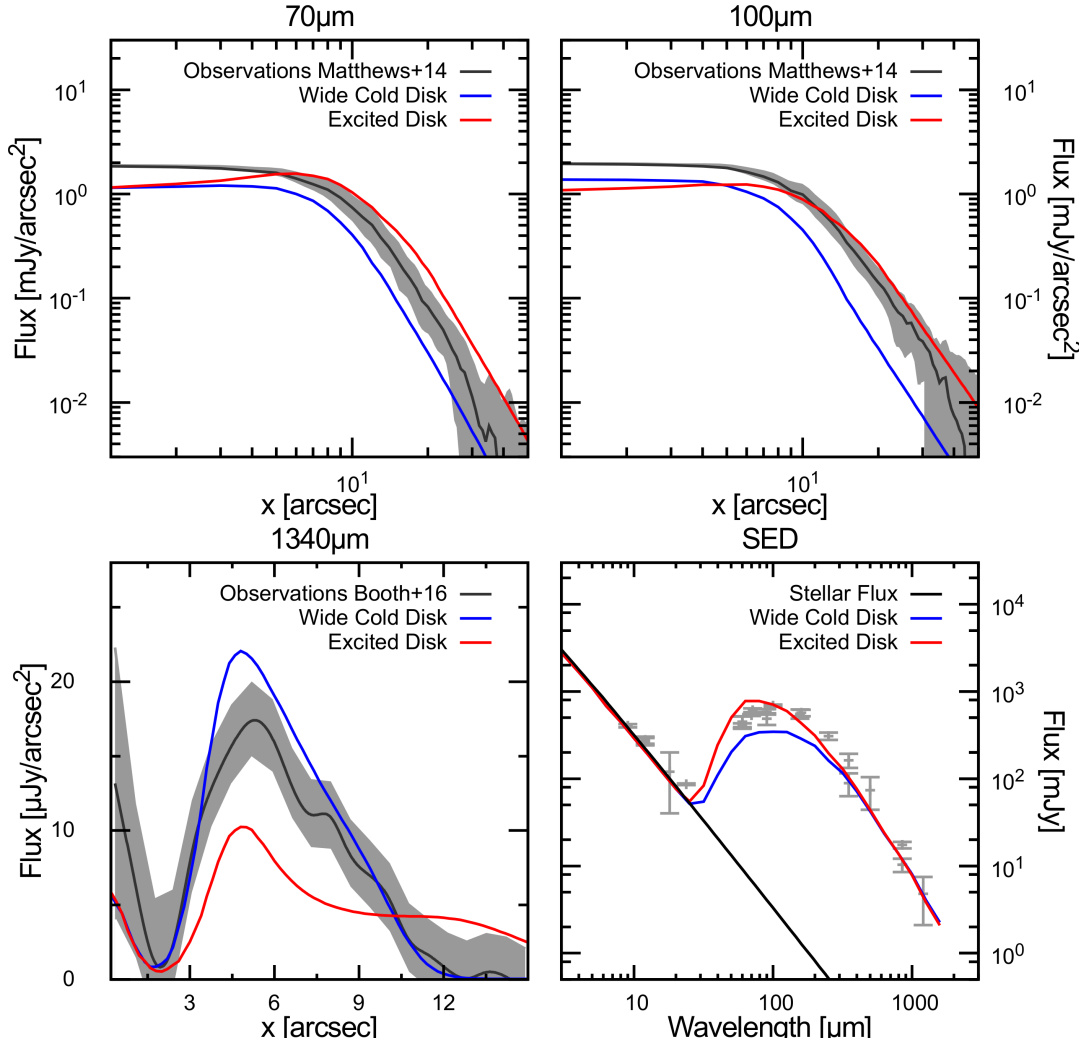


Figure 2. Profiles and the SED for the wide cold disc and an excited disc model. Black: observations and error bars (in grey). Red: the excited disc model with a belt at 360 – 440 AU and an eccentricity of 0.5 – 0.6. Blue: a debris disc with planetesimals from 150 AU to 440 AU with eccentricities up to 0.1.

for the strength regime, $b_g = 1.38$, $Q_{D,g} = 1 \times 10^{-6}$ for the gravity regime, and $v_0 = 3 \text{ km s}^{-1}$ are in accordance with the values found in Benz & Asphaug (1999). We included disruptive, cratering and bouncing collisions in our runs. Collisions are considered catastrophic when the impact energy exceeds the specific disruption energy Q_D^* as described in Stewart & Leinhardt (2009) and Löhne et al. (2012). Cratering of the larger collider occurs when impact energy suffices only to disrupt the smaller collider. For even lower impact energies remnants of both colliders may bounce off each other. Fragments of all these types of collisions are assumed to follow a mass distribution with number density proportional to $m^{-1.83}$, the average found in Fujiwara et al. (1977) and Fujiwara (1986).

3.3 Collisional age of the system

To model the disc we need its collisional age, the time since the start of destructive collisions, which we assume to be roughly equal to the system's age. HR 8799's age remains a strongly debated topic and values from around 30 Myr (Zuckerman et al. 2011; Baines et al. 2012; Bell et al. 2015) up to 1 Gyr (Moya et al. 2010) exist in the literature. Most estimates, however, give an age between 30 Myr

and 100 Myr with one line of reasoning being HR 8799's membership of the Columba moving group (Torres et al. 2008; Zuckerman et al. 2011; Bell et al. 2015) which sets the age closer to 30 – 40 Myr. We have checked the probability of HR 8799 being a member of Columba with the Banyan Σ code (Gagné et al. 2018) using the latest astrometry from Gaia's 2nd data release (Gaia Collaboration et al. 2018) and a radial velocity of $-12.6 \pm 1.4 \text{ km/s}$ (Gontcharov 2006). We find a Columba membership probability of 48.7%, much lower than that found by previous analyses using pre-Gaia data (Zuckerman et al. 2011; Malo et al. 2013; Read et al. 2018), casting into doubt the likelihood of membership. We therefore conclude that the age cannot currently be better determined than $60_{-30}^{+100} \text{ Myr}$ (Marois et al. 2008). We adopt this age for all further simulations.

4 MODELLING AND RESULTS

With simulation runs taking up to several days and a great amount of parameters to vary, choosing the parameters for each run and improving a model is done on a trial-and-error basis rather than systematically covering a range of parameters. As such, the pro-

cess of finding a well fitting model is always subject to some educated guesses. This means that, although a well fitting model may be found, other solutions might be possible.

4.1 Excited disc

In the first step we placed the initial planetesimals in orbits with high semimajor axes and high eccentricities, such that the periastra of these orbits lie between 140 – 220 AU. With this we tried to produce a halo of larger grains to address the problems we found with the Herschel/PACS based model. We varied the eccentricities and semimajor axes in tandem, while trying to reproduce the observations. We again show an example (red lines in Fig. 2) which illustrates the problems with this setup. Comparison with the PACS data shows that now we find dust far enough out in the system to reproduce the halo mentioned in Matthews et al. (2014), and even overshoot in the 70 μm image. We pay for this by underestimating the profile height significantly further in. It is even clearer when comparing to the ALMA profile, where the disc is very faint compared to the observation. This is because the optical depth distribution is much flatter as orbits with high eccentricities distribute the dust over a larger area. Although collisions occur in the pericentre, more mass is needed for there to be enough mass close to the star. The SED on the other hand tells us that we need less material contradicting the other profiles. Up to this point we did not yet consider the high eccentricities and where they originated. At a loss to explain the high eccentricities or to solve the mass distribution contradictions we conclude that this model is unable to create the halo and to match the brightness levels of the radial profiles.

4.2 Wide cold disc

In the next step we used a wide cold disc of planetesimals, following the same idea as Booth et al. (2016), and evolved it collisionally. We tried different low values of eccentricity, initial masses and the position of the disc and in the end settled for values only marginally different from those in Booth et al. (2016). We set the innermost periastra of the initial distribution to be close to the inner edge of the disc at 145 AU, since that edge was well resolved in the ALMA data. Since the parameters found here are not unique either, the difference between the two sets of parameters can be neglected. Just as before, we calculated the radial profiles and SEDs and compared them to the observations in Fig. 2. An example of such a model is seen in blue, with its parameters in Tab. 2. Although this is only an example, its shortcomings are present in all the other similar models we tried. The PACS images reveal the first major problem: this disc is not extended far enough. In both the 70 and the 100 μm image the profile fits nicely in the inner region but falls literally short further out. It is important to note here that radiation pressure is not effective enough to create the halo seen in the observations. Neither bound nor unbound grains are abundant enough at these distances. This contradicts the previous models of Su et al. (2009) and Matthews et al. (2014). The synthetic ALMA image shows a higher peak than the observations, while the SED is too low. So the profiles at different wavelengths give us different remedies for the model. We can either increase the total mass to better reproduce the PACS profiles or reduce the total mass to better reproduce the ALMA profiles. Another problem in this step is that we again have to explain destructive collisions at large distances and as such we need a mechanism of stirring the planetesimals to explain our value of $e = 0.1$. Together with the other problems encountered, this leads

us to conclude that the wide cold disc model cannot reproduce the observations.

4.3 Synthesis model

We find that a single population is insufficient to reproduce the radial profiles, as the models show that high eccentricities are needed to create the extended emission and low eccentricities needed to reproduce the profile heights. Catering to both, we tried a synthesis model of both approaches, an excited population and a wide cold population. The excited population would resemble a scattered disc. Explaining the broad disc of HR 8799 with a scattered disc has, in fact, previously been suggested by Wyatt et al. (2017) who note that this would be a natural result of the proposed fifth planet. The parameters were chosen in such a way that in all variations the pericenters of the innermost orbits reach to 130 AU. The total masses of these two populations were varied independently, but the same radial slope for the optical depth was assumed. Additionally we set a warm component between 6 – 8 AU with a mass needed to adjust the underpredicted 24 μm photometry. The contribution of such a warm component to the profiles is negligible except for the innermost part of the ALMA profile. The peak there can be explained by the flux of the warm component and the star.

Starting again with the PACS images, we see that this model reproduces the outer slope of the profile while filling the inner regions of the disc. The preferred model manages to recreate the slope in the outer regions, although in the 70 μm image (Fig. 3) we produce a bit too much flux further out. We plotted the contribution of both populations separately by only calculating the image with objects with $e < 0.3$ and another image with objects with $e \geq 0.3$. The radial profile of these images shows that the excess of flux stems from the overlap of the two populations. Removing this excess is rather difficult due to the interconnectedness of the different images. Since the error we have in the image is rather small, we are content with the profiles. By setting the outer edge closer to the star one can reduce the profile height at all PACS wavelengths but also the flux in the slope. We did not find a configuration of two populations that could solve this problem entirely. At this point we want to stress, however, that our model for the scattered disc is rather crude and a more nuanced model could alleviate this (see section 5.1). The 1340 μm profile in Fig. 3 also fits the observations rather well. In summary we see a less severe version of the same problem as in the excited disc model: we overestimate the flux at shorter wavelengths, which is also reflected by the SED. The model reproduces the profiles to satisfaction, with a few minor discrepancies.

5 DISCUSSION

5.1 Comparison to the Kuiper belt

We found that both models of Matthews et al. (2014) and Booth et al. (2016), while explaining their respective observation, fail once applied to other wavelengths. The collisional simulations also showed that, for the parameters tested (which cover a large, although not exhaustive, range), single population discs failed to reproduce the profiles. The model most closely reproducing the disc incorporates two populations of parent bodies, with one of them being dynamically excited. This configuration is roughly similar to the Kuiper Belt of our Solar System with a population of objects of low eccentricity and a scattered population with higher eccentricities (Fig. 4). The slight differences in the observations and the

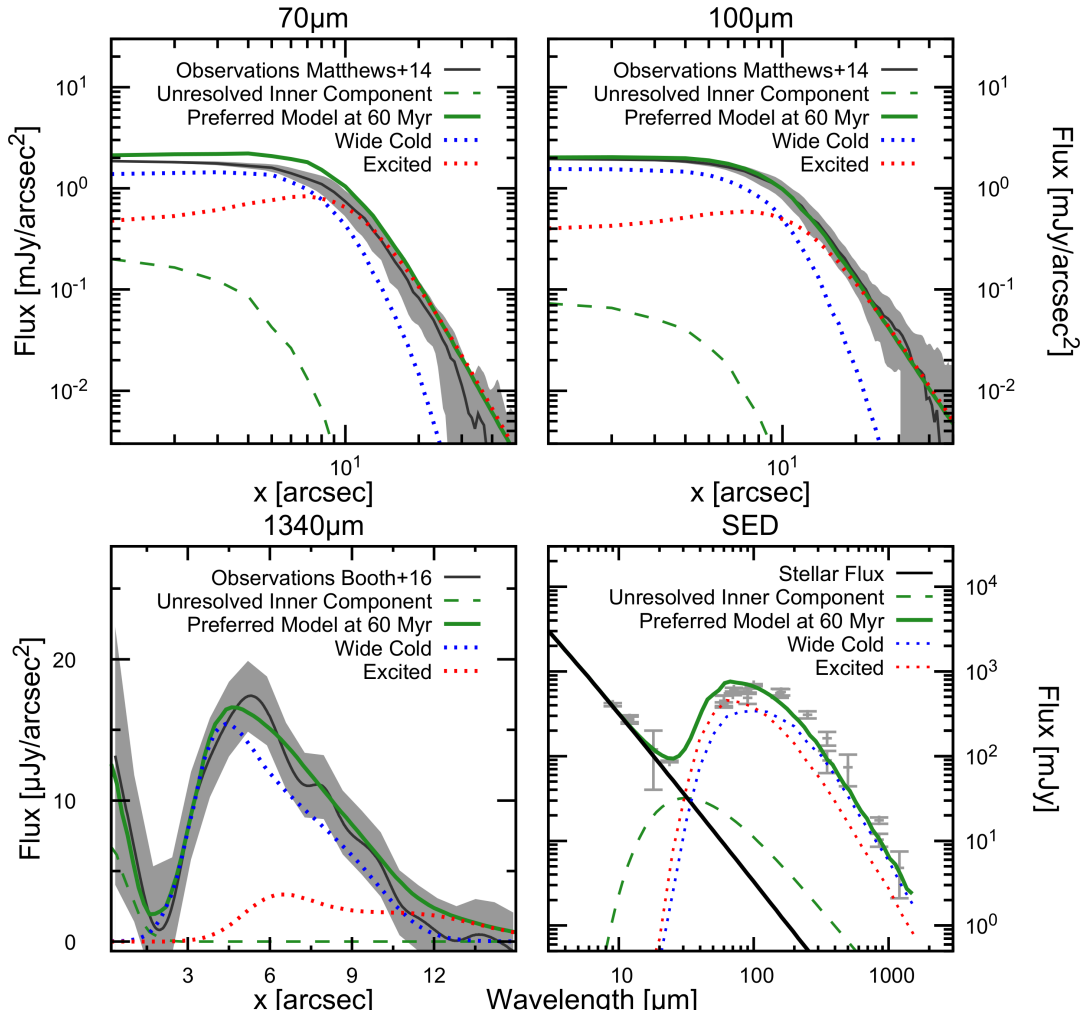


Figure 3. Profiles and the SED for the preferred scattered disc model. Black: observations and error bars (in grey). Green: The preferred model, comprising the star, the inner component, a wide cold disc and a excited one, drawn in a solid line. The unresolved inner component was additionally plotted with a dashed line. Red and Blue: The individual populations plotted with a dotted line.

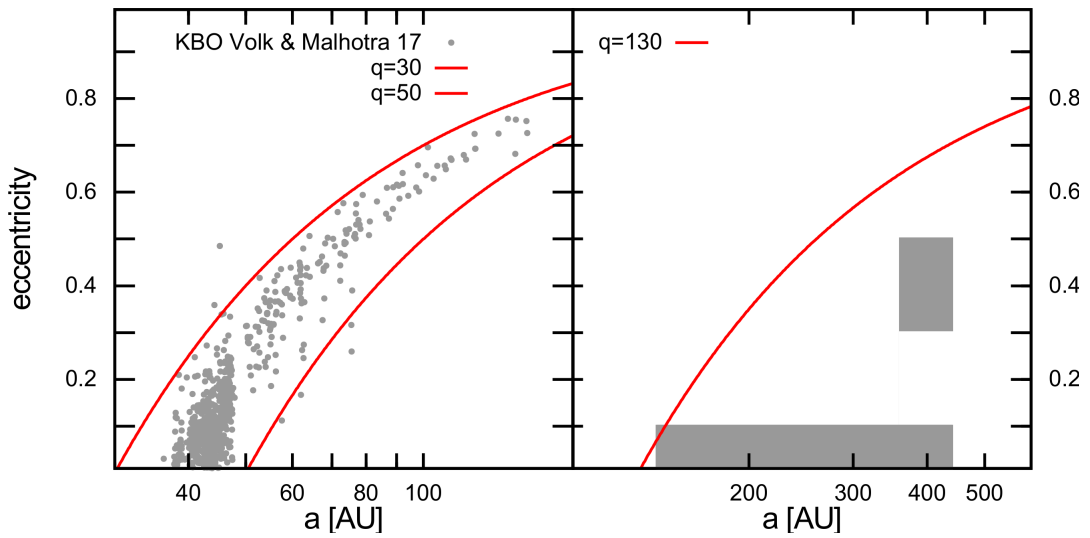


Figure 4. Left: Kuiper Belt population from Volk & Malhotra (2017) in the a - e -plane with rough boundaries. Right: Population of our preferred model with the inner edge of the disc as boundary. This comparison highlights that our model, while similar in approach, is missing the complexity of the continuous distribution of the Kuiper Belt.

model can be explained with the restrictions we have with our code. While in reality the transition from the low eccentricity population to the high eccentricity one is smooth, we are bound by our grid of orbital parameters. With only two populations used we already almost double the number of the disc parameters in the code. To describe a scattered disc adequately, the amount of parameters would be too unwieldy to obtain any satisfactory solution in any reasonable amount of time. Although the observed inner edge of the disc serves as a rough approximation of the periastron and restricts the parameter range (see Fig. 4), we still have the masses and many a - e -configurations to consider.

5.2 New SMA data

In the work of [Wilner et al. \(2018\)](#) new SMA observations of HR 8799 at 1340 μ m were published and, in contrast to [Booth et al. \(2016\)](#), the visibilities were fitted. With this fitting technique, the inner edge of the debris disc appears to be at around 110 AU with the disc extending to around 500 AU. This aligns the inner edge more with the Herschel observations. By moving the cold population closer to the star, we can adjust the inner edge, but the inability to explain the halo with just radiation pressure still persists. Therefore, our conclusion that a scattered disc is the best explanation for the observations does not change with a closer inner edge.

5.3 Origin of the scattered disc

The proposed scattered disc can be created in many different ways. In the Kuiper Belt it is believed to be the result of the migration of the giant planets ([Gomes et al. 2018](#); [Kaib & Sheppard 2016](#)), and similar evolutionary paths were suggested for the giant planets in HR 8799 ([Marois et al. 2010](#); [Patience et al. 2011](#); [Dodson-Robinson et al. 2009](#)). To discuss its origin, we first look at the masses in the two components in the preferred model and their implications for the protoplanetary disc and planet formation. We find an initial mass of $133M_{\oplus}$ for the extended population, and $67M_{\oplus}$ for the scattered population with planetesimals up to the size of 100 km. Assuming the scattered population originated as part of the extended population, we calculate the protoplanetary disc mass by assuming that the distribution of the material in the currently observed disc held further-in at the preceding protoplanetary phase. The resulting total mass of solids is $270M_{\oplus}$, of which $200M_{\oplus}$ are bound in the disc and $70M_{\oplus}$ resided in the region currently occupied by four giant planets. This mass would have been enough for the planet cores to form, yet the high mass of the scattered population poses the question of the scattering mechanisms.

Recently, a fifth planet has been suggested by [Read et al. \(2018\)](#) to explain the location of the inner edge of the debris disc as seen in [Booth et al. \(2016\)](#). Modelling its influence on the evolution of the debris disc with N-body simulations, [Read et al. \(2018\)](#) found a planet with a mass of $0.1M_{\text{Jup}}$ ($\sim 30M_{\oplus}$) and a semi-major axis of 138 AU to best explain the shape of the ALMA profile of ([Booth et al. 2016](#)). Could that planet, if real, be the cause of the scattered disc? [Wyatt et al. \(2017\)](#) studied the typical outcomes of close encounters between planets and orbit-crossing planetesimals. Applying their results to the fifth planet shows that it would scatter most of the orbit-crossing material onto bound orbits, thus supporting the fifth planet as the cause of the scattered disc. However, this planet's mass of $\sim 30M_{\oplus}$ is much lower than the mass of the scattered population ($\sim 70M_{\oplus}$). It is impossible that a much less massive planet scattered the much more massive planetesimal population. [Read et al. \(2018\)](#) furthermore found that planets with a

mass in the range from $1M_{\text{Jup}}$ to $0.04M_{\text{Jup}}$ corresponding to either a semimajor axis from 115 AU to 130 AU or from 140 AU to 160 AU, with the most massive planets being nearest to or farthest away from the star, similarly well explained the observations. Although any planet with a mass in excess of $0.8M_{\text{Jup}}$ would eject orbit-crossing material, a fifth planet capable of scattering $\sim 70M_{\oplus}$ of planetesimals is still possible.

As the fifth planet may or may not be real, we shift our focus on to the four confirmed planets. Referring again to the work by [Wyatt et al. \(2017\)](#), one sees that the gas giants of HR 8799, each for itself, would typically eject their orbit-crossing material in unbound orbits. This material would be on its way out of the system, but, unless this is a continuous process, it should only operate for a relatively short amount of time. For this process to be continuous, a constant flux of material would need to cross the giant planet's path, which is unlikely. Therefore we do not consider scattering through the giant planets to be responsible for the scattered disc either.

Migration is considered to have occurred in the formation history of HR 8799, as neither core accretion nor gravitational instability could have produced all four planets at their current location ([Currie et al. 2011](#)). Although we focus in the discussion on outward migration a similar case can be made for inward migration. Using the formula of [Ida et al. \(2000\)](#) to calculate the migration rate in our primordial disc, we find a rate of a few 10s of AU/Myr. Such a fast migration would allow the planets to quickly reach their current location. Taking into account that migration stops when the mass within a few Hill radii becomes less than the planet's mass ([Kirsh et al. 2009](#)), we find the fully formed planets in HR 8799 to be too massive to have undergone migration within the protoplanetary disc. However, if the planets accreted their gas envelope while migrating or even after the migration ceased, then the core masses rather than planet masses would have to be considered. Migration rate of these, less massive, cores would be lower, and they could easily create a scattered disc of planetesimals instead of ejecting them out of the system.

Planet-planet scattering may have also occurred early on in the history of the HR 8799 system. If the planet cores formed closer to the star by core accretion, such a scattering event could have relocated the planets, bringing them to their current location. If the planets acquired their gas envelopes after the scattering event, it is possible that the debris disc circularised their orbits, which must have been made eccentric by scattering ([Bromley & Kenyon 2011](#); [Currie et al. 2011](#)), through dynamical friction of the planet with planetesimals (e.g., [Thommes et al. 1999](#)). Obviously it is much easier to circularise the cores than the fully formed gas giants.

The discussion above hinges on the mass estimates we obtain from our model. It is possible to get larger (smaller) masses by increasing (decreasing) the maximum planetesimal size of 100 km, while maintain the same collisional evolution. However only a change of an order of magnitude has an impact on the overall mass large enough to change our conclusions. For a less massive disc a fifth planet as proposed in [Read et al. \(2018\)](#) becomes more plausible. More massive discs slow migration more effectively and one therefore has to consider how far a planet core migrates.

5.4 Other systems

A natural question is, whether the scattered disc is unique for HR 8799 or can be typical of other debris disc systems. A distinct feature of the HR 8799 disc is its large radial extent seen in the (sub-)mm images. This disc has a relative width $\Delta r/r \approx 1$, where Δr and r are the disc's radial extent and mean radius, respectively.

It is natural to expect that potential scattered disc-hosting systems are those that, like HR 8799, appear extended at (sub-)mm wavelengths. We analysed a list of 26 debris discs that have been resolved with ALMA or SMA compiled by [Matrà et al. \(2018\)](#). One of them is HR 8799 itself. We inspected the other 25 systems of the list and found 10 discs to have a relative width $\Delta r/r > 0.8$. With 11 out of 26 systems being “extended” by this criterion, scattered discs could be a common feature. As a caveat, many of these systems have a second dust belt, which impedes a correct determination of the belt width.

As discussed above, formation of scattered discs require planets to be present in the systems. Considering the same sample of discs from [Matrà et al. \(2018\)](#), [Krivov & Booth \(2018\)](#) checked which of them do require planets as stirrers to explain the dust production. They found three such discs: HR 8799, HD 95086 and 49 Cet. While HD 95086 does have one directly imaged planet with a large gap to the inner edge of the disc ([Rameau et al. 2013](#)), planets around 49 Cet are still waiting to be discovered ([Choquet et al. 2017](#)). Given the fact that the discs in these two systems are extended and the planets there are either known or at least strongly suspected, we propose them to be particularly good candidates for hosting scattered discs.

6 CONCLUSIONS

In this work we considered models for the cold debris disc of HR 8799 proposed by [Matthews et al. \(2014\)](#) and [Booth et al. \(2016\)](#). The former is based on Herschel observations and the latter on ALMA 1.34mm data. We confirmed that both of them reproduced the observation they were based on adequately, but we found them to fail when applied to the other observations. We then searched for a model explaining both sets of observations. To this end, we used the ACE code to collisionally evolve an initial distribution of planetesimals. The resulting dust distribution was then taken to calculate a set of synthesized images to compare to the observations. Our findings are as follows:

- (i) Neither a wide planetesimal disc nor an excited narrow disc are able to reproduce the observations, when including radiation pressure, indicating that radiation pressure is not able to reproduce the observed halo.
- (ii) A two-population model with a cold debris disc and a scattered population of planetesimals fits the observations of HR 8799 the best. This architecture is similar to our own Solar System’s Kuiper Belt with its classical and scattered components, suggesting its origin to also be similar.
- (iii) A scattered population may be a common feature of debris discs, and probably forms by planets interacting with the disc. For HR 8799 we discussed planet-planet scattering events and migration scenarios involving four to five planets. We believe that the proposed fifth planet can be massive enough to have created the scattered population. The known four planets are too massive to have created a bound scattered population via migration. However, a bound scattered population could have been created by the planet cores through their migration and scattering, if such events occurred before the gas accretion onto the cores.

7 ACKNOWLEDGEMENTS

We thank the anonymous reviewer for their helpful comments and suggestions. This research was supported by the DFG, grants Kr 2164/13-1, Kr 2164/15-1 and Lo 1715/2-1.

REFERENCES

- Baines, E. K., White, R. J., Huber, D., et al. 2012, *ApJ*, 761, 57
- Bell, C. P. M., Mamajek, E. E., & Naylor, T. 2015, *Proceedings of the International Astronomical Union*, 10, 41-48
- Benz, W. & Asphaug, E. 1999, *Icarus*, 142, 5
- Booth, M., Jordán, A., Casassus, S., et al. 2016, *MNRAS*, 460, L10
- Boss, A. P. 1997, *Science*, 276, 1836
- Bromley, B. C. & Kenyon, S. J. 2011, *Astrophys. J.*, 735, 29
- Brott, I. & Hauschildt, P. H. 2005, in *ESA Special Publication*, Vol. 576, *The Three-Dimensional Universe with Gaia*, ed. C. Turon, K. S. O’Flaherty, & M. A. C. Perryman, 565
- Brown, R. L., Wild, W., & Cunningham, C. 2004, *Advances in Space Research*, 34, 555
- Burns, J. A., Lamy, P. L., & Soter, S. 1979, *Icarus*, 40, 1
- Chatterjee, S., Ford, E. B., Matsumura, S., & Rasio, F. A. 2008, *ApJ*, 686, 580
- Chen, C. H., Sargent, B. A., Bohac, C., et al. 2006, *ApJS*, 166, 351
- Choquet, É., Milli, J., Wahhaj, Z., et al. 2017, *ApJ*, 834, L12
- Cohen, M., Wheaton, W. A., & Megeath, S. T. 2003, *Astron. J.*, 126, 1090
- Crida, A. 2009, *Astrophys. J.*, 698, 606
- Currie, T., Burrows, A., Itoh, Y., et al. 2011, *ApJ*, 729, 128
- Dodson-Robinson, S. E., Veras, D., Ford, E. B., & Beichman, C. A. 2009, *ApJ*, 707, 79
- Draine, B. T. 2003, *Ann. Rev. Astron. Astrophys.*, 41, 241
- Duncan, M., Quinn, T., & Tremaine, S. 1989, *Icarus*, 82, 402
- Eiroa, C., Marshall, J. P., Mora, A., et al. 2013, *Astron. Astrophys.*, 555, A11
- Fabrycky, D. C. & Murray-Clay, R. A. 2010, *Astrophys. J.*, 710, 1408
- Fujiwara, A. 1986, *Memorie della Societa Astronomica Italiana*, 57, 47
- Fujiwara, A., Kamimoto, G., & Tsukamoto, A. 1977, *Icarus*, 31, 277
- Gagné, J., Mamajek, E. E., Malo, L., et al. 2018, *ApJ*, 856, 23
- Gaia Collaboration, Brown, A. G. A., Vallenari, A., et al. 2018, *A&A*, 616, A1
- Gomes, R., Nesvorný, D., Morbidelli, A., Deienno, R., & Nogueira, E. 2018, *Icarus*, 306, 319
- Gontcharov, G. A. 2006, *Astronomy Letters*, 32, 759
- Goździewski, K. & Migaszewski, C. 2009, *MNRAS*, 397, L16
- Goździewski, K. & Migaszewski, C. 2014, *MNRAS*, 440, 3140
- Goździewski, K. & Migaszewski, C. 2018, *ApJS*, 238, 6
- Gray, R. O., Corbally, C. J., Garrison, R. F., McFadden, M. T., & Robinson, P. E. 2003, *Astron. J.*, 126, 2048
- Helou, G. & Walker, D. W., eds. 1988, *Infrared astronomical satellite (IRAS) catalogs and atlases. Volume 7: The small scale structure catalog*, Vol. 7
- Heng, K. & Tremaine, S. 2010, *MNRAS*, 401, 867
- Høg, E., Fabricius, C., Makarov, V. V., et al. 2000, *Astron. Astrophys.*, 355, L27
- Holland, W. S., Matthews, B. C., Kennedy, G. M., et al. 2017, *MNRAS*, 470, 3606
- Hughes, A. M., Wilner, D. J., Andrews, S. M., et al. 2011, *Astrophys. J.*, 740, 38
- Ida, S., Bryden, G., Lin, D. N. C., & Tanaka, H. 2000, *ApJ*, 534, 428
- Ishihara, D., Onaka, T., Katata, H., et al. 2010, *A&A*, 514, A1
- Jura, M., Chen, C. H., Furlan, E., et al. 2004, *Astrophys. J. Suppl.*, 154, 453
- Kaib, N. A. & Sheppard, S. S. 2016, *AJ*, 152, 133
- Kenyon, S. J. & Bromley, B. C. 2008, *Astrophys. J. Suppl.*, 179, 451
- Kenyon, S. J. & Bromley, B. C. 2009, *Astrophys. J.*, 690, L140
- Kirsh, D. R., Duncan, M., Brasser, R., & Levison, H. F. 2009, *Icarus*, 199, 197
- Krivov, A. V. & Booth, M. 2018, *MNRAS*, 479, 3300

- Krivov, A. V., Eiroa, C., Löhne, T., et al. 2013, *Astrophys. J.*, 772, 32
- Krivov, A. V., Löhne, T., & Sremčević, M. 2006, *A&A*, 455, 509
- Lasker, B. M., Lattanzi, M. G., McLean, B. J., et al. 2008, *Astron. J.*, 136, 735
- Li, A. & Greenberg, J. M. 1998, *Astron. Astrophys.*, 331, 291
- Löhne, T., Augereau, J.-C., Ertel, S., et al. 2012, *A&A*, 537, A110
- Maldonado, J., Eiroa, C., Villaver, E., Montesinos, B., & Mora, A. 2012, *Astron. Astrophys.*, 541, A40
- Malo, L., Doyon, R., Lafrenière, D., et al. 2013, *ApJ*, 762, 88
- Marois, C., Macintosh, B., Barman, T., et al. 2008, *Science*, 322, 1348
- Marois, C., Zuckerman, B., Konopacky, Q. M., Macintosh, B., & Barman, T. 2010, *Nature*, 468, 1080
- Marshall, J. P., Moro-Martín, A., Eiroa, C., et al. 2014, *Astron. Astrophys.*, 565, A15
- Matrà, L., Marino, S., Kennedy, G. M., et al. 2018, *ApJ*, 859, 72
- Mathews, B., Kennedy, G., Sibthorpe, B., et al. 2014, *ApJ*, 780, 97
- Meshkat, T., Mawet, D., Bryan, M. L., et al. 2017, *AJ*, 154, 245
- Monet, D. G., Levine, S. E., Canzian, B., et al. 2003, *Astron. J.*, 125, 984
- Moór, A., Ábrahám, P., Derekas, A., et al. 2006, *Astrophys. J.*, 644, 525
- Moore, A., Hasan, I., & Quillen, A. C. 2013, *MNRAS*, 432, 1196
- Moro-Martín, A., Malhotra, R., Bryden, G., et al. 2010, *Astrophys. J.*, 717, 1123
- Moro-Martín, A., Marshall, J. P., Kennedy, G., et al. 2015, *ApJ*, 801, 143
- Moshir, M., Kopan, G., Conrow, T., & 9 colleagues. 1990, *IRAS Faint Source Catalogue*, version 2.0.
- Moya, A., Amado, P. J., Barrado, D., et al. 2010, *MNRAS*, 405, L81
- Patience, J., Bulger, J., King, R. R., et al. 2011, *Astron. Astrophys.*, 531, L17+
- Pearce, T. D. & Wyatt, M. C. 2014, *MNRAS*, 443, 2541
- Perryman, M. A. C., Lindegren, L., Kovalevsky, J., et al. 1997, *Astron. Astrophys.*, 323, L49
- Poglitsch, A., Waelkens, C., Geis, N., et al. 2010, *Astron. Astrophys.*, 518, L2
- Pollack, J. B., Hubickyj, O., Bodenheimer, P., et al. 1996, *Icarus*, 124, 62
- Rameau, J., Chauvin, G., Lagrange, A.-M., et al. 2013, *Astrophys. J. Lett.*, 772, L15
- Read, M. J., Wyatt, M. C., Marino, S., & Kennedy, G. M. 2018, *MNRAS*
- Reidemeister, M., Krivov, A. V., Schmidt, T. O. B., et al. 2009, *Astron. Astrophys.*, 503, 247
- Rhee, J. H., Song, I., Zuckerman, B., & McElwain, M. 2007, *Astrophys. J.*, 660, 1556
- Sadakane, K. & Nishida, M. 1986, *PASP*, 98, 685
- Skrutskie, M. F., Cutri, R. M., Stiening, R., et al. 2006, *Astron. J.*, 131, 1163
- Stewart, S. T. & Leinhardt, Z. M. 2009, *Astrophys. J. Lett.*, 691, L133
- Su, K. Y. L., Rieke, G. H., Stapelfeldt, K. R., et al. 2009, *Astrophys. J.*, 705, 314
- Sylvester, R. J., Skinner, C. J., Barlow, M. J., & Mannings, V. 1996, *MNRAS*, 279, 915
- Thommes, E. W., Duncan, M. J., & Levison, H. F. 1999, *Nature*, 402, 635
- Torres, C. A. O., Quast, G. R., Melo, C. H. F., & Sterzik, M. F. 2008, *Young Nearby Loose Associations*, 757
- Volk, K. & Malhotra, R. 2017, *AJ*, 154, 62
- Williams, J. P. & Andrews, S. M. 2006, *Astrophys. J.*, 653, 1480
- Wilner, D. J., MacGregor, M. A., Andrews, S. M., et al. 2018, *ApJ*, 855, 56
- Wisdom, J. 1980, *Astron. J.*, 85, 1122
- Wyatt, M. C., Bonsor, A., Jackson, A. P., Marino, S., & Shannon, A. 2017, *MNRAS*, 464, 3385
- Wyatt, M. C., Kennedy, G., Sibthorpe, B., et al. 2012, *MNRAS*, 424, 1206
- Yamamura, I., Makiuti, S., Ikeda, N., et al. 2010, *VizieR Online Data Catalog*, 2298
- Zacharias, N., Monet, D. G., Levine, S. E., et al. 2004, *BAAS*, 36, 1418
- Zuckerman, B., Rhee, J. H., Song, I., & Bessell, M. S. 2011, *ApJ*, 732, 61
- Zuckerman, B. & Song, I. 2004, *Astrophys. J.*, 603, 738